Processes Controlling the Mean Tropical Pacific Precipitation Pattern. Part I: The Andes and the Eastern Pacific ITCZ

KEN TAKAHASHI AND DAVID S. BATTISTI

Department of Atmospheric Sciences, University of Washington, Seattle, Washington

(Manuscript received 12 May 2006, in final form 6 October 2006)

ABSTRACT

The question of why the intertropical convergence zone (ITCZ) is generally north of the equator in the tropical Pacific is addressed. Experiments with an atmospheric general circulation model coupled to idealized representations of the ocean show that the presence of the Andes is enough to lower sea surface temperature (SST) off the west coast of South America through evaporation, thus promoting a north–south asymmetry, with the ITCZ north of the equator, which is amplified by interactions between the ocean and the atmosphere. The evaporative cooling results mainly from the subsidence of low specific humidity air, which is due in turn to the mechanical effect of the Andes on the zonal mean flow. The positive feedback from low-level clouds on SST is an important factor for the efficiency of the mechanism described.

West of 120°W, the presence of the Rockies and Himalayas produces a comparable forcing to that of the Andes, but this is not enough to reverse or neutralize the north–south asymmetry set by the Andes. It is shown that the longitudinal offset between the forcings in both hemispheres allows the Andes to preferentially set the north–south asymmetry, which propagates westward into the rest of the Pacific.

Asymmetry in the observed ocean heat transports (more heat transport convergence in the Northern Hemisphere) associated with the Kuroshio was found to reinforce the effect of the Andes, although it is not a strong forcing by itself. Sensitivity experiments indicate that the north–south asymmetry of the ITCZ caused (evaporatively) by the Andes is robust to the presence of a strong equatorial cold tongue and to seasonality in insolation.

1. Introduction

A striking characteristic of the mean climatic state of the tropical Pacific is that the intertropical convergence zone (ITCZ) is generally located to the north of the equator. The ITCZ is associated with an underlying sea surface temperature (SST) that is higher than that in the Southern Hemisphere (SH) at the same latitudes (Fig. 1). An explanation for this north–south asymmetry cannot be found in the external forcing of the earth system, that is, insolation, since it is essentially symmetric about the equator, with the exception of a slight bias toward the SH, which should produce the opposite asymmetry from what is observed. Therefore, asymmetries within the system must be responsible for the asymmetry in the longitudinal position of the Pacific ITCZ. The fluid dynamics of the ocean and atmosphere do not predict a preference for either hemisphere, so the northern location of the ITCZ can ultimately be explained only by the geography of the continents and oceans.

An important piece of the puzzle was provided by Xie and Philander (1994, hereafter XP94), who described a mechanism by which air–sea interactions in a simplified model allowed stable equilibrium states with the ITCZ in one hemisphere and colder water in the other. This so-called wind–evaporation–SST (WES) mechanism assumes that convection occurs preferentially over warm water and that, if it is initially stronger in one hemisphere, it would then drive stronger surface wind speeds in the other hemisphere, which would cool the water there by evaporation, reinforcing the initial location of the convection. That this asymmetry is a stable state of their unforced system (and that the symmetric state is unstable) indicates that the forcing required to select either of the two possible asymmetric configurations need not be very strong. Wang and Wang (1999), using a somewhat more complex model, found that the symmetric state in their model was stable

Corresponding author address: Ken Takahashi, NOAA/Geophysical Fluid Dynamics Laboratory, Princeton, NJ 08540.
E-mail: ken.takahashi@noaa.gov

DOI: 10.1175/JCLI4198.1

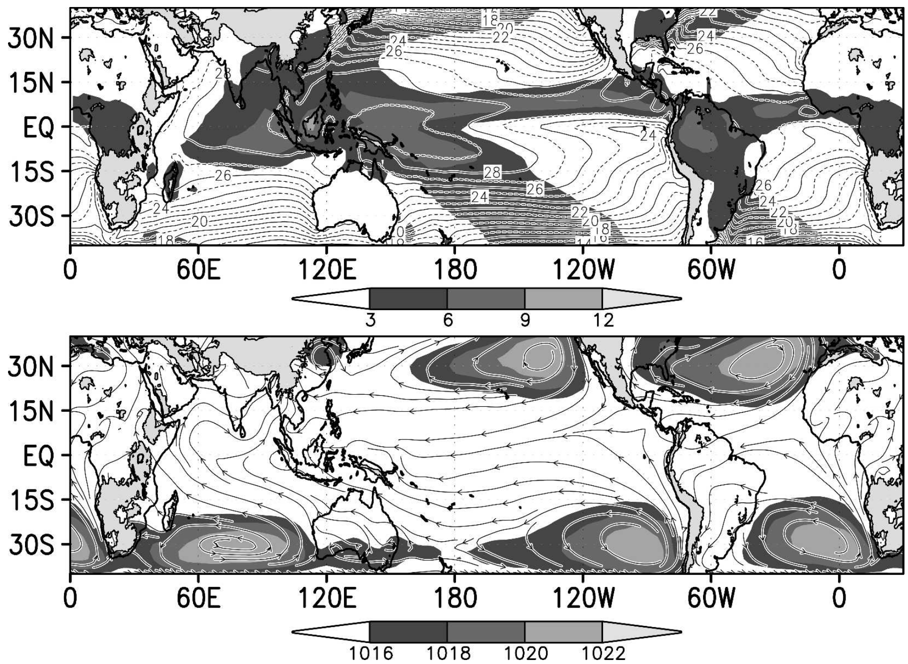

Fig. 1. (top) Climatological mean rainfall rate (shaded; mm day^{-1}; data from the Global Precipitation Climatology Project; Huffman et al. 1997) and SST (contours; °C; data from NCEP OI SST v2; Reynolds et al. 2002). (bottom) Climatological mean 925-mb streamlines and mean sea level pressure (shaded; mb) from NCEP–NCAR reanalysis (Kalnay et al. 1996; Kistler et al. 2001). Land elevation greater than 1000 m is lightly shaded and bounded by a thin contour.

under equinoxial insolation. When the seasonal cycle of insolation was included in their model, the two asymmetric states, similar to those of XP94, became the stable states.

Philander et al. (1996, hereafter P96) addressed the question of what causes the Pacific climate to be dominated by a single ITCZ that is located north of the equator. Using general circulation models (GCMs), they concluded that the most important geographical asymmetry was that the orientation of the coastline of South America is more favorable for coastal upwelling than the one of North and Central America. This, they argued, would cool the SH preferentially and drive the climate system into an asymmetric state with the ITCZ north of the equator. Interestingly, their coupled ocean–atmosphere model produced only a weak asymmetry and they argued that the feedback from low-level clouds, ubiquitous in the southeastern Pacific (Mitchell and Wallace 1992; Klein and Hartmann 1993, hereafter KH93) but absent from their model, might be a crucial ingredient that could enhance the asymmetry. A difficulty with the P96 hypothesis is the mismatch of scales: coastal upwelling has a spatial scale of about 50 km, whereas the observed low SST region has a much larger scale, as discussed below.

A different result was obtained by Giese and Carton (1994), who also ran a coupled GCM under very similar conditions but obtained a stronger north–south asymmetry in the eastern Pacific than P96, even though the coastal SST off South America in their model was among the highest in the Pacific, indicating a serious misrepresentation of coastal cooling processes, such as upwelling. Their model also had deficiencies in low-level clouds, but a fundamental difference from the P96 study was that they considered realistic topography, whereas P96 had flat land only. Altogether, the above results suggest that a process involving mountains, different from coastal upwelling, might be acting to create the observed north–south asymmetry.

An examination of the climatological SST distribution off the coast of South America (Fig. 1) reveals two distinct cool regions: a narrow coastal one off Peru (coolest around 15°S) directly associated with coastal upwelling (e.g., Takahashi 2005), and a broad cold region extending from the central coast of Chile (around 30°S) toward the northwest, and to about 3000 km offshore. We hypothesize that the latter results from the presence of the South Pacific subtropical anticyclone, which cools the ocean surface through evaporation, effectively suppressing deep convection in the Southern

Hemisphere and leading to the northerly location of the ITCZ. As argued by Rodwell and Hoskins (2001; hereafter RH01), the Andes, to a large extent, force the subtropical southeastern Pacific anticyclone into place. However, farther to the west a similar, although weaker, cool region can be seen extending to the southwest from the coast of California (Fig. 1). A crucial asymmetry is that there is no counterpart to this system in the Northern Hemisphere (NH) *at the same longitudes* and this allows the north–south asymmetry to develop in the eastern basin and propagate westward (Xie 1996), where the forcing by the NH anticyclone, which is "downstream" of the SH anticyclone, is unable to reverse it.

In this paper, we will test our hypotheses within the context of a numerical model, and the processes responsible for the north–south asymmetry will be investigated. The following section will describe the numerical models used. Section 3 will assess the effect of the presence of the Andes on local SST and in driving the north–south asymmetry. In section 4, the effects of the Rockies and Himalaya, as well as of the asymmetry in ocean heat transport, will be assessed. Section 5 presents additional experiments to test the importance of low-level cloud feedback and the robustness of the effect of the Andes to the presence of a strong equatorial cold tongue and seasonality. Finally, further discussion of the results and conclusions will be presented.

2. Models

a. Atmosphere

The model used is based on a primitive-equation dynamical core with T63 spectral truncation and seven vertical levels and a suite of simplified physical parameterization schemes optimized for this vertical resolution (Molteni 2003). The climatology of a T30 version of this model, forced with observed SST, is reasonably realistic in the tropical Pacific, comparable to many state-of-the-art general circulation models (Molteni 2003).[1]

A limitation of the model that is potentially important is the misrepresentation of low stratiform clouds in subtropical subsidence regions, which play a crucial role in mean tropical climate (KH93; Mechoso et al. 1995). Therefore, a scheme for the diagnosis of the cover associated with these clouds was implemented based on the linear relation between cloud cover (CC) and low-level stability found by KH93 (see the appendix).

The only orography used in the experiments was that associated with the Andes, the Rockies, and the Himalaya (Fig. 2). The Andes required special considerations due to their narrowness, which, at the T63 truncation, produced a strong Gibbs effect. This had the consequence of producing large undulations in the surface height over the ocean, with amplitudes of up to 500 m, which significantly affected the surface heat fluxes. To ameliorate this effect, the Andes were widened by approximately 50% in the zonal direction, while maintaining the height unchanged. This reduced the amplitude of the undulations to around 100 m, with extreme values of around −200 m (Fig. 2). This procedure should not affect the representation of interaction between the Andes and the flow over the southeast Pacific, since the mechanism is nonlinear and consists mainly on blocking of the westerly flow (RH01), which is a function of the height and not the width of the mountains. This is supported by idealized experiments, reported in more detail in Takahashi and Battisti (2007, hereafter Part II), which indicate that the subsidence rate is insensitive to the width of the Andes.

When orography was included, only the surfaces of the mountain ranges were considered to be land (Fig. 2). On these, the temperature was fixed and given the value of the reference SST distribution adjusted by a "surface" lapse rate of 4.8°C km^{-1}, which was estimated from observational data.[2] This lapse rate was considered instead of one representative of the free troposphere because the way isentropes intersect the surface appears to be an important factor for the interaction of the large-scale flow and the mountains in subsidence regions (RH01). The soil moisture was set to zero, so the mountains do not act as moisture sources.

Unless otherwise stated, the runs were made with annual mean insolation symmetrical about the equator. All coupled runs are 10 yr long and the averages from the last 6 yr are shown. The runs with fixed SST were 48 months long, and we show the averages from the last 40 months.

An aquaplanet run (AQUA) with no orography and fixed (reference) SST was performed to calculate both the Q-fluxes required for the mixed layer model (see next section) and a reference atmospheric state for the

[1] We used T63 instead of the original T30 spectral truncation to better resolve the Andes and to improve the representation of the midlatitude westerly flow, which is sensitive to resolution (e.g., Held and Phillips 1993).

[2] The land temperature climatology is from the Climatic Research Unit (CRU) of the University of East Anglia; the orography is from the 5-min gridded elevation (ETOPO5) dataset obtained from the National Geophysical Data Center of the National Oceanic and Atmospheric Administration (NOAA).

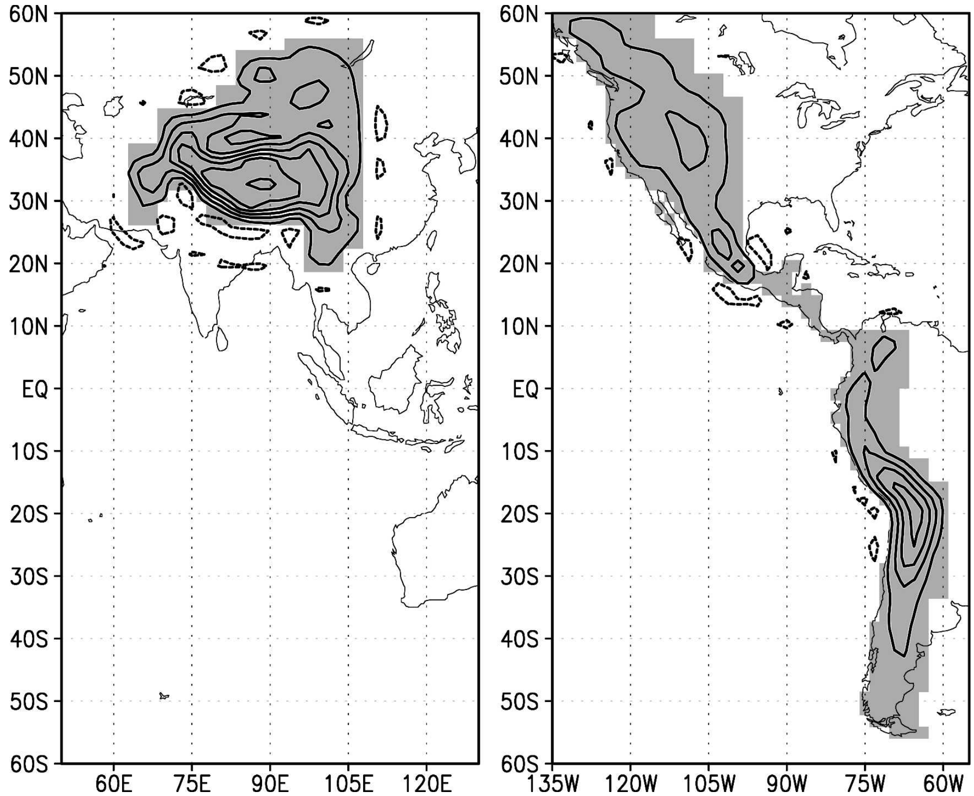

FIG. 2. Topography for the Andes, Rockies, and Himalayas used in the experiments (solid contours every 1000 m with zero omitted for clarity, and −100-m contour dashed). The shaded areas are treated as land.

analysis in section 3c. The resulting zonal mean precipitation from this run features a double ITCZ, with peaks of around 7 mm day^{-1} at approximately 7° latitude (Fig. 3). The surface heat fluxes peak at the equator with values similar to observational estimates (cf. dashed and dotted curves in Fig. 3), although the model produces much stronger fluxes into the tropical ocean off the equator. This model bias is associated with a shortwave (SW) bias of around 30 W m^{-2} at the top of the atmosphere, which implies a planetary albedo of around 0.2, two-thirds of the observed. This, in turn, appears to be associated with biases in cloud albedo, which are particularly strong in the off-equatorial Tropics.

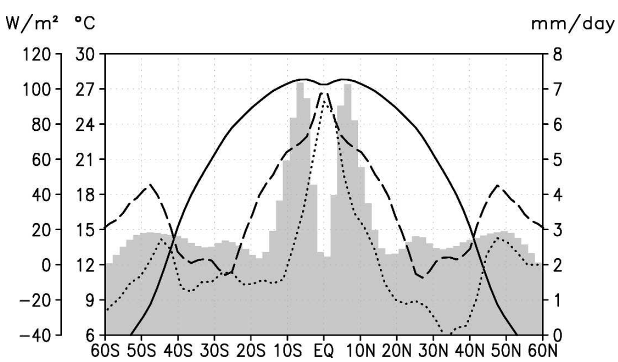

FIG. 3. Reference SST distribution (solid line; °C), and zonal mean precipitation (shaded; mm day^{-1}) and net surface heat flux (dashed line; W m^{-2}) from the AQUA run. Also, an estimate of the zonal average surface heat flux for the Pacific Ocean based on data from NCEP–NCAR reanalysis (Trenberth and Caron 2001) assuming a basin width of 140° longitude (dotted).

b. Ocean

The ocean was represented in a highly simplified manner. Between 40°S and 40°N, either SST was prescribed to match the reference distribution, which consisted of the zonal- and annual-mean SST symmetrized about the equator (Fig. 3), or an interactive mixed layer (ML) was used, forced by the net surface heat fluxes produced by the atmospheric model and prescribed Q-fluxes that are symmetric about the equator and constant in longitude. Poleward of 40°, SST was prescribed.

The temperature T in the interactive mixed layer is determined by the heat budget equation:

$$C\frac{dT}{dt} = \text{SW} + \text{LW} + \text{LHF} + \text{SHF} + Q, \qquad (1)$$

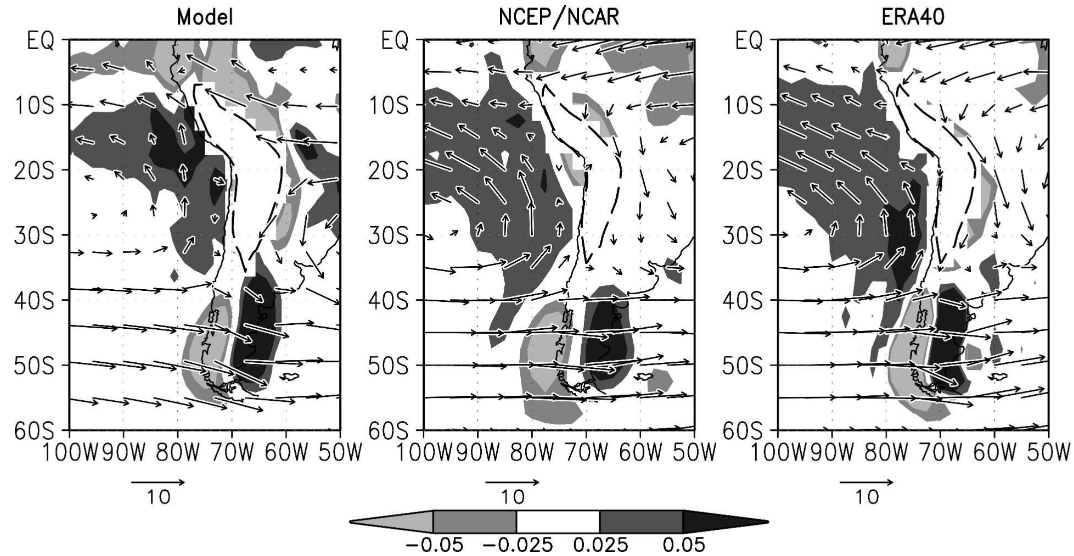

FIG. 4. 850-mb pressure velocity (Pa s^{-1}, shaded) and horizontal wind (m s^{-1}) from the (left) ANDES_FIXED run, (middle) NCEP–NCAR reanalysis, and (right) ERA-40. The 850-mb surface isobar is dashed. Spatial smoothing was applied to the vertical motion field in the left panel.

where SW and LW are the net surface shortwave and longwave (LW) radiative fluxes, respectively, LHF and SHF are the net surface latent and sensible heat fluxes (LHFs and SHFs), respectively, and C is the heat capacity of the mixed layer, taken to be 50 m deep.

The Q-fluxes (Q), which act as a proxy for the effect of ocean heat transports, were determined from the zonal and temporal averages of the net surface heat flux from the AQUA run (Fig. 3), symmetrized about the equator. Since, in equilibrium, the Q-fluxes must balance this surface heat flux, the former are estimated by multiplying the latter by -1.

3. Effect of the Andes

a. Experiment 1: Fixed SST

To assess the direct effect of the Andes on the otherwise equatorially and zonally symmetric atmospheric flow seen in the AQUA run, we run the model with the same aquaplanet configuration but including the Andes. In this experiment (ANDES_FIXED) the only orography is that shown in Fig. 2 over South America and only the surface of these mountains was considered to be land. SST was prescribed to match the reference distribution, so ocean–atmosphere interactions are not present.

The resulting distribution of low-level horizontal and vertical motion around the Andes features the five centers of vertical motion described by RH01 as the signature of nonlinear adiabatic interaction between the zonal mean flow and mountains (cf. our Fig. 4, left, and Fig. 12 in RH01), except for an additional region of strong ascent on the eastern flank of the Andes north of 20°S in our model (Fig. 4, left), which is associated with deep convection. The distribution of 850-mb vertical motion is remarkably similar to the vertical motion field in the National Centers for Environmental Prediction–National Center for Atmospheric Research (NCEP–NCAR) reanalysis and 40-yr European Centre for Medium-Range Weather Forecasts (ECMWF) Re-Analysis (ERA-40; Fig. 4, center and right). The horizontal flow is also very similar, although the equatorward flow is weaker in our model (Fig. 4). According to the theory of RH01, the subtropical subsidence is essentially adiabatic and is a result of the blocking of the westerly flow by the Andes, which is then deflected equatorward along the downward-sloping isentropes (RH01). However, in the Tropics, radiative cooling plays an important role in compensating for the warming due to subsidence. Following RH01, the vertical and horizontal advective tendencies of potential temperature at 600 mb from our results are shown in Fig. 5; evident in these figures is the presence of nearly adiabatic descent poleward of 20°S (where vertical and horizontal advection cancel one another) and diabatic descent equatorward of that latitude (where horizontal advection is unimportant).

Within the oceanic subsidence region, surface cooling is enhanced by around 30 W m^{-2} in the region 20°–10°S, 90°–80°W (Fig. 6, left), of which about 80% is due to the enhancement of the latent heat fluxes (Fig. 6, right).

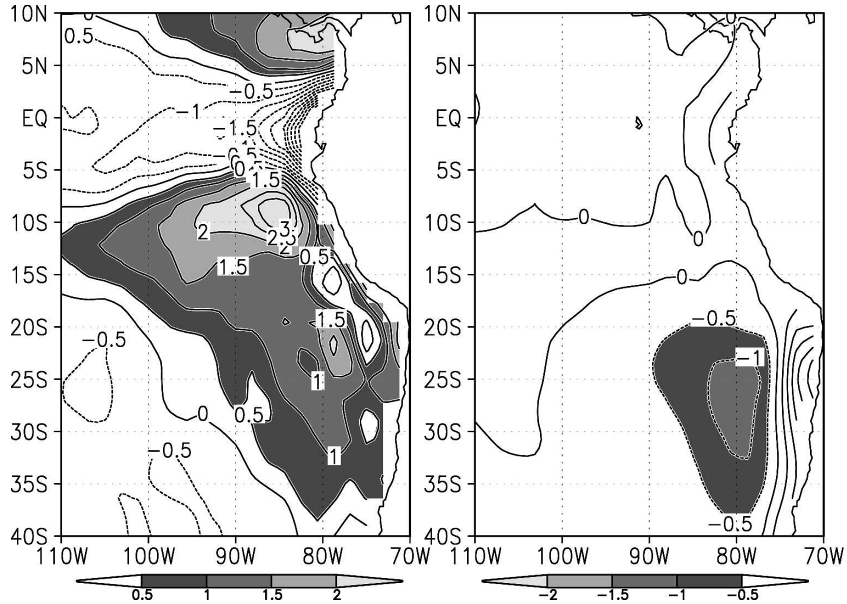

FIG. 5. Difference in (left) vertical and (right) horizontal advective tendencies of potential temperature (10^{-5} K s^{-1}) at 600 mb between the ANDES_FIXED and the AQUA runs. Note the reversal in shading scheme. Spatial smoothing was applied to both fields.

The increase in evaporative cooling appears to be the result of the combination of the drying of the boundary layer (Fig. 6, left) and the enhancement of surface wind speed[3] (Fig. 6, right). It is of particular interest to determine whether the drying is due to advection of drier air from aloft or from higher latitudes. In Fig. 7 we show the advective tendencies of specific humidity calculated at 887.5 mb. Between 20° and 5°S, where the descent is diabatic, the dominant term is vertical advection of dry air. On the other hand, poleward of 20°S, both terms are of similar magnitude, albeit small. These results suggest that most of the drying in the boundary layer is due to the enhancement in subsidence rate.

Interestingly, despite the drying effect of the Andes on the low-level conditions in the southeast Pacific, the southern branch of the ITCZ was enhanced in this experiment (Fig. 8), presumably due to the enhancement in moisture influx associated with the strengthening of the southerly flow due to the Andes. Also, the influence of the Andes on the rainfall distribution extends westward only to 120°W. However, as shown in the next section, coupling to the ocean changes this dramatically.

[3] The trade winds are very steady (e.g., Riehl 1979), so the magnitude of the mean vector wind provides an approximate measure of wind speed.

b. *Experiment 2: Interactive mixed layer*

The perturbation in surface heat fluxes associated with the presence of the Andes will produce changes in the surface temperature of the ocean, which in turn will affect the atmospheric circulation. In particular, it is expected that the ocean west of the Andes will cool, leading to a suppression of convection in this region and to a north–south asymmetry with the ITCZ in the NH. To test this idea, we performed an experiment (ANDES), similar to the previous one, except that the atmosphere interacts with the ML ocean model instead of fixed SST.

The results exhibit a strong north–south asymmetry in precipitation throughout the Pacific. In the east Pacific, east of the date line, a single ITCZ is located north of the equator (Fig. 9, top), which is significantly more intense than those in the AQUA case. Farther to the west, a weaker ITCZ is also found in the SH. Interestingly, the results feature a realistically located South Pacific convergence zone (SPCZ), although it is narrower and less horizontally tilted than the observed (cf. Figs. 1 and 9, top). The processes controlling the SPCZ and the geometry of the dry zone to the east of it are addressed in Part II.

Associated with this equatorial asymmetry, SST is reduced in the southeast Pacific with respect to the reference state by as much as 3.5 K, with the cooling extending into the equatorial region, producing a weak equatorial cold tongue (Fig. 9, top).

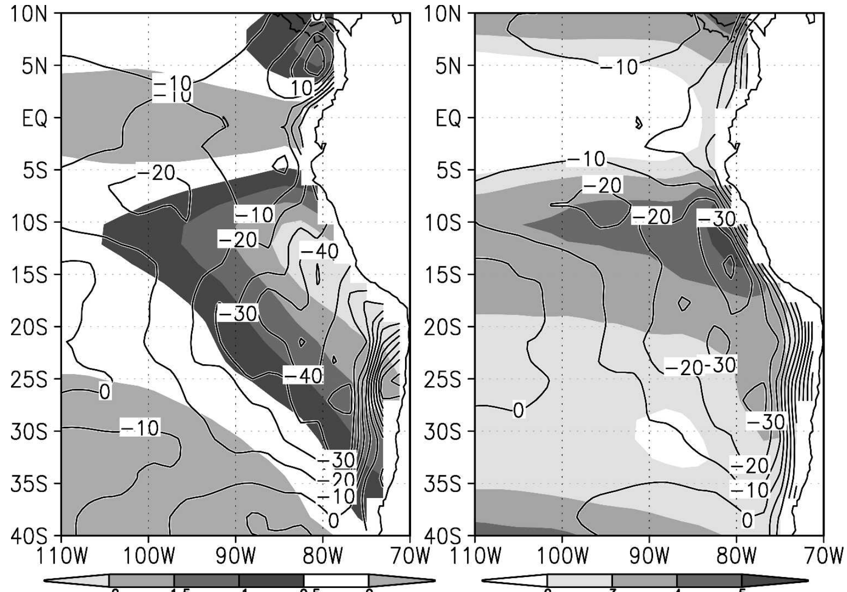

FIG. 6. Difference in (left) 925-mb specific humidity (g kg^{-1}; shaded) and net surface heat flux (W m^{-2}; contours) and (right) magnitude of the surface wind vector (m s^{-1}; shaded) and surface latent heat flux (W m^{-2}; contours) between the ANDES_FIXED and the AQUA runs. Spatial smoothing was applied to all fields.

The eastern flank of the South Pacific anticyclone is realistic (cf. Figs. 1 and 9, bottom), and the equatorward flow is strengthened by the presence of the mountains (by $\sim$4 m s^{-1} within approximately 1000 km of the coast), with respect to the AQUA run. The low-level flow features a northward component on the equator throughout the Tropics, which is presumably a consequence of the westward propagation of the north–south asymmetry (Xie 1996; Xie and Saito 2001).

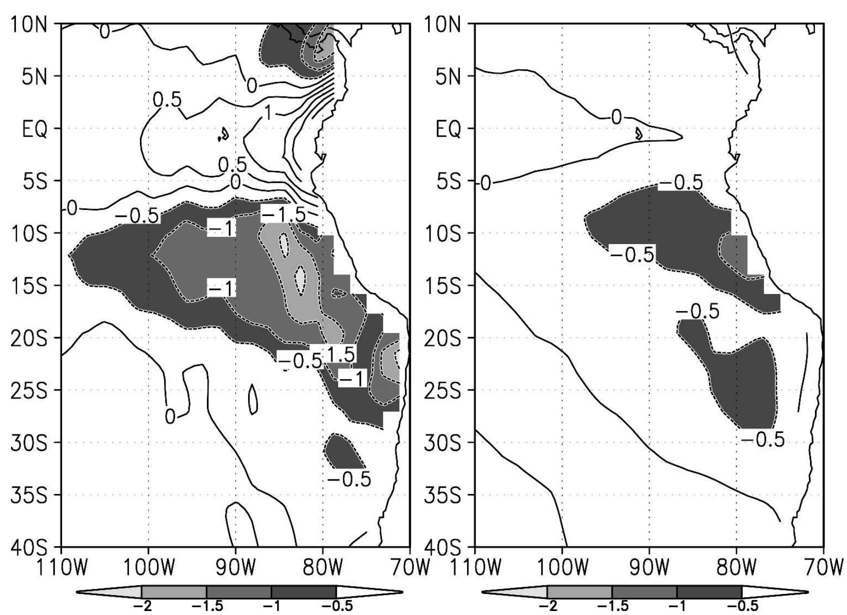

FIG. 7. (left) Vertical and (right) horizontal advective tendencies of specific humidity (10^{-5} g kg^{-1} s^{-1}) at 887.5 mb in the ANDES_FIXED run. Spatial smoothing was applied to both fields.

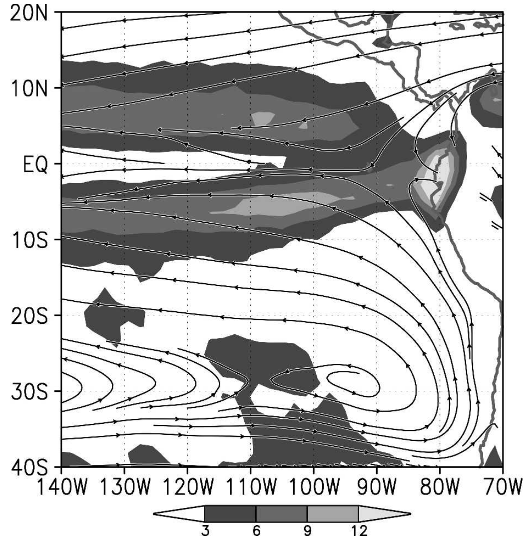

FIG. 8. Precipitation (shading; mm day^{-1}) and 925-mb streamlines in the ANDES_FIXED run.

c. *Surface heat flux analysis*

To diagnose the mechanism through which the presence of the Andes forces the north–south asymmetry in the eastern Pacific, we will start by comparing the individual components of the surface heat flux. Table 1 presents the averaged SST and surface fluxes from the ANDES run averaged over four regions. The SH_{off} box (20°–10°S, 90°–80°W; see Fig. 9 for location of the boxes) corresponds to the maximum surface cooling and the NH_{off} box covers the same latitudinal and longitudinal range but in the opposite hemisphere (10°–20°N, 90°–80°W). The NH_{eq} box corresponds to the region occupied by the ITCZ in the NH (5°–10°N, 140°–100°W), while the SH_{eq} box covers the same latitudes and longitudes in the opposite hemisphere (10°–5°S, 140°–100°W).

The area averages of the SST and surface heat flux components, shown in Table 1 as departures from the corresponding zonal mean and hemispherically symmetrized fluxes from the AQUA run, are discussed next.[4]

It can be seen that there is a general cooling in the eastern Pacific, but the changes in the SH SST are larger than in the NH. In general, the changes in the components of the surface heat flux are small. In the off-equatorial box in the NH (NH_{off}) the changes are negligible in general, while in the NH ITCZ (NH_{eq})

[4] The small negative residual in the budgets (on the order of 1 W m^{-2}) indicates that equilibrium was nearly, but not fully, achieved.

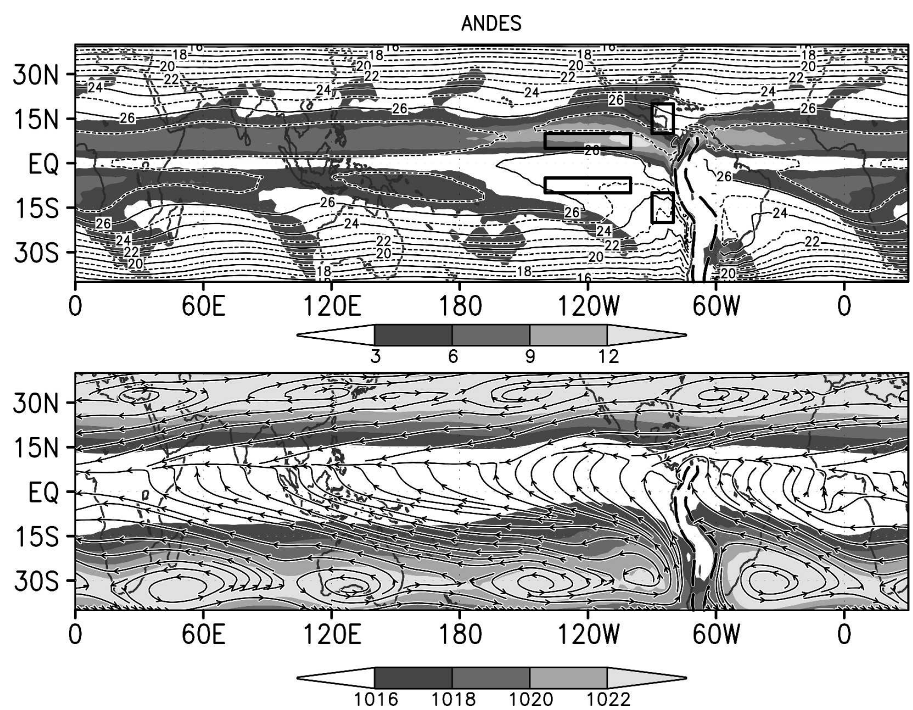

FIG. 9. (top) Mean rainfall rate (shading; mm day^{-1}) and SST (contours; °C) for the ANDES run. (bottom) Mean sea level pressure (shading; mb) and 925-mb streamlines for the ANDES run. In both panels, the intersection of the surface with the 925-mb isobar is indicated by the dashed contour. The coastlines are included for reference only. The boxes are described in the text.

TABLE 1. Area-averaged deviations in SST (°C) and net surface SWs, LWs, LHFs, and SHFs (W m^{-2}) for the ANDES minus AQUA run. Fluxes are positive into the ocean. See the text for the location of the boxes.

Box	ΔSST	ΔSW	ΔLW	ΔLHF	ΔSHF
NH_{off}	−0.2	1.3	−1.4	0.7	−1.4
NH_{eq}	−1.3	−14.7	7.2	6.9	0.3
SH_{eq}	−2.6	11.4	−8.2	−3.7	0.0
SH_{off}	−3.3	−7.2	−2.5	6.0	2.9

there seems to an increase in shading from insolation by convective clouds, which is compensated by reduced evaporative and longwave cooling.

In the SH_{eq} box, the reduction in convective clouds leads to an increase in insolation, which is mostly compensated by increased longwave cooling and, to a lesser extent, by evaporation. However, changes in net longwave cooling at the surface in the Tropics act as a positive feedback through changes in water vapor (Hartmann and Michelsen 1993), so it is not obvious what drives the cooling in the first place.

The question of what drives the cooling is particularly relevant to the off-equatorial box (SH_{off}), where the strongest cooling is found. The changes in heat fluxes are relatively small and the balance is mainly between decreased insolation and reduced evaporative cooling. Naively interpreted, this might suggest that the presence of stratus clouds is responsible for the cooling. However, these clouds act mainly as a feedback on SST rather than as a forcing (e.g., Philander et al. 1996; Takahashi 2005). As we will show next, despite its small change in equilibrium, it is evaporation that produces the reduction in SST.

d. Diagnosis of the forcing of SST

To assess the relative importance of different processes in the determination of the surface cooling in the SH due to the introduction of the Andes, we will consider the changes in the equilibrium energy budget of the ocean mixed layer:

$$\Delta \mathrm{SW} + \Delta \mathrm{LW} + \Delta \mathrm{LHF} + \Delta \mathrm{SHF} = 0, \quad (2)$$

where Δs indicate differences between the run with Andes (ANDES) and without (AQUA). Note that, by construction, $\Delta Q = 0$.

As an approximation, we write the changes in radiative fluxes as a forcing plus a feedback on SST changes:

$$\Delta \mathrm{SW} + \Delta \mathrm{LW} = \Delta F + \gamma \Delta T, \quad (3)$$

where ΔF is an externally imposed radiative forcing (e.g., the impact of the Andes on the downward longwave forcing at the surface by reducing free troposphere moisture) and γ is a radiative feedback parameter, which includes the effects of low-level clouds and the water vapor feedback. As we will see, the actual value of γ is of no consequence to the following analysis.

We use the following bulk formulas[5] for representing latent and sensible heat fluxes:

$$\mathrm{LHF} = -L_v C_e \rho U(q_s - q) \quad (4)$$

$$\mathrm{SHF} = -c_p C_s \rho U(T - T_a), \quad (5)$$

where T stands for SST, T_a for surface air temperature, C_e and C_s are the exchange coefficients, U is the surface wind speed, q is the near-surface specific humidity, and q_s is the near-surface saturation specific humidity. For our analysis we will assume $L_v C_e$, $c_p C_s$, and ρ to be constants.

Substituting into (2), we get

$$\Delta F + \gamma \Delta T - \Delta L_v C_e \rho U(q_s - q) - \Delta c_p C_s \rho U(T - T_a) = 0. \quad (6)$$

As we saw in the run with fixed SST (section 3a), the presence of the Andes changes the low-level circulation near the surface, which implies changes in near-surface wind speed, as well as in temperature and specific humidity of the air masses advected into the Tropics. Although there is a strong influence from the ocean on air temperature and specific humidity through sensible heat flux and evaporation, respectively, the changes in these variables are ultimately determined by the changes in the atmospheric circulation. Therefore, we will consider the changes in U, q, and T_a, together with ΔF, as manifestations of the external "forcings" (land or mountains).

Assuming small changes, we make a linear approximation of (6):

[5] The linear dependence of our bulk formulas on wind speed, instead of quadratic, is consistent with the formulation of the atmospheric model.

$$\Delta F + \gamma \Delta T - L_v C_e \rho \left\{ U_r \left[\left(\frac{\partial q_s}{\partial T} \right)_r \Delta T - \Delta q \right] + (q_{sr} - q_r)\Delta U \right\} - c_p C_s \rho (U_r(\Delta T - \Delta T_a) + (T_r - T_{ar})\Delta U) = 0, \quad (7)$$

which can be rewritten using (4) and (5) as

$$\Delta T = \alpha_r \left(-\frac{\Delta U}{U_r} + \frac{1}{1 + B_r} \frac{\Delta q}{q_{sr} - q_r} + \frac{B_r}{1 + B_r} \frac{\Delta T_a}{T_r - T_{ar}} - \frac{\Delta F}{(1 + B_r)\mathrm{LHF}_r} \right), \quad (8)$$

where

$$\alpha_r \equiv (1 + B_r)\left[\frac{\gamma}{\mathrm{LHF}_r} + \frac{1}{q_{sr} - q_r}\left(\frac{\partial q_s}{\partial T}\right)_r + \frac{B_r}{T_r - T_{ar}}\right]^{-1} \tag{9}$$

and $B \equiv \mathrm{SHF/LHF}$ is the Bowen ratio. The subscript r indicates the reference state (corresponding to the AQUA run). Equation (8) enables us to estimate the change in SST (ΔT) associated with changes in the atmospheric variables ultimately due to the presence of the mountains. Although estimating the actual value of ΔT would require determining α_r, at this point we are only interested in the relative importance of the processes represented by ΔU, Δq, and ΔT_a in changing SST through the latent and sensible heat fluxes and the direct effect of ΔF, which can be assessed by comparing the four terms in the parentheses on the rhs of (8) (U term, q term, T_a term, and F term, respectively).

The values of these terms calculated over the same SH boxes as for Table 1, are shown in Table 2. We roughly estimated the F term, corresponding to longwave radiative forcing associated with the changes in upper-tropospheric humidity produced by the presence of the Andes, by taking $\Delta F \approx \Delta \mathrm{LW}$ from Table 1, while $\Delta \mathrm{SW}$ is assumed to participate only as a feedback.[6]

In the $\mathrm{SH_{off}}$ box, which experiences the most direct forcing from the mountains, the dominant process is, by far, drying (q term), which contributes 92% of the cooling (Table 2). This indicates that, in our experiment, the means by which the presence of the Andes, and the resulting subtropical anticyclone, cools the ocean is by drying the tropical near-surface boundary layer. It should be noted that these results do not imply that low-level clouds are not important for the cooling near the continent: since they act as a feedback, their contribution is through the term involving γ in α_r [defined in (9)].

In the $\mathrm{SH_{eq}}$ box, where the SH ITCZ was obliterated by the presence of the Andes, the cooling is produced mainly by the increase in wind speed (56% of the cooling), but also to a significant extent by the drying effect (37%). XP94 argued that the changes in wind speed are the dominant factor in setting up the north–south asymmetry, but our results suggest that the effects of changes in specific humidity are also important.

[6] In the uncoupled run (ANDES_FIXED), ΔLW is somewhat stronger in the $\mathrm{SH_{off}}$ box (-6 W m^{-2}), which indicates that it participates in a negative feedback to the ocean cooling. However, the results are qualitatively unchanged and the effect on T remains small. In the $\mathrm{SH_{eq}}$ box we do not expect a direct forcing by the Andes, so our estimate for the F term provides an upper bound.

TABLE 2. Area-averaged relative contributions to SST changes, through latent and sensible heat fluxes, by changes in surface wind speed (U term), in specific humidity (q term), in surface air temperature (T_a term), and by changes in radiative fluxes (F term).

Box	U term	q term	T_a term	F term
$\mathrm{SH_{eq}}$	−1.3	−0.9	−0.1	−0.1
$\mathrm{SH_{off}}$	0.1	−1.4	−0.2	−0.0

The simplest model for how the SST is changed in the $\mathrm{SH_{off}}$ box, based on the previous results, is one in which evaporative cooling associated with dry air advection cannot be balanced, in equilibrium, except by the lowering of SST, which decreases the evaporation rate:

$$\Delta \mathrm{LHF} = -L_v C_e \rho U(\Delta q_s - \Delta q) \approx 0, \tag{10}$$

which, in the linear approximation, leads to

$$\Delta T = \left(\frac{\partial q_s}{\partial T}\right)^{-1} \Delta q. \tag{11}$$

Using the Clausius–Clapeyron equation with a temperature of 300 K and a pressure of 1000 mb, we obtain $\Delta T \approx 0.8\Delta q$, where T is in Kelvins and q is in g kg^{-1}. In fact, we can see an excellent spatial correlation between the ΔT and Δq fields (Fig. 10), and linear regression analysis for the region 35°S–0°, 120°–80°W for the model yields $\Delta T \approx 0.7\Delta q$, which is close to what is obtained from (11).

It is worth noting that, if we consider separately the two Δ terms in (10) and take $\Delta q_s = \Delta q = 3$ g kg^{-1} (cf. Fig. 10), the magnitude of each term is on the order of 100 W m^{-2}. Therefore, the net change in latent heat fluxes shown in Table 1 results from the cancellation

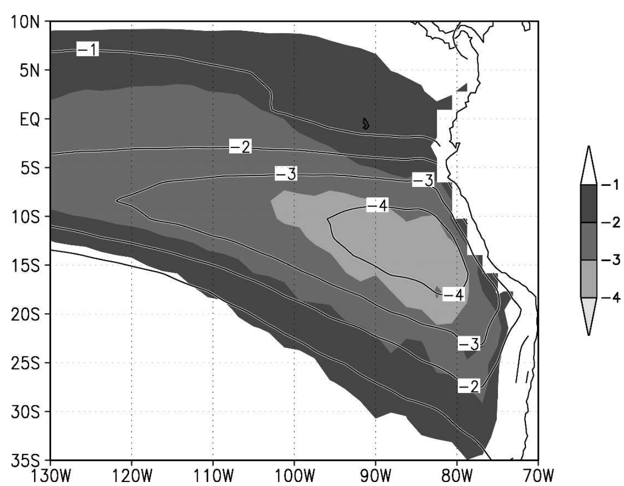

FIG. 10. Difference in SST (shaded; K) and 925-mb specific humidity (contours, g kg^{-1}) between the ANDES and the AQUA runs.

between two large terms and does not reflect the importance of evaporation in producing the changes in SST.

The above considerations can be summarized in a more intuitive way by considering the adjustment process to the instantaneous introduction of the Andes. Dry air from above is forced to subside and is entrained into the boundary layer over the ocean to the west of the Andes, thereby strongly enhancing surface evaporative cooling. As the upper ocean cools, the efficiency with which it does so decreases with the saturation vapor pressure according to the Clausius–Clapeyron equation (the strongest negative feedback), although, as indicated next, this reduction is significantly offset by the increase in low-level clouds, which blocks insolation and, thus, allows the cooling to proceed further. When equilibrium is reached, however, the net change in evaporation is small because the initial increase in evaporation is tempered by the reduction in the surface saturation vapor pressure (due to lower SST).

Note that if we include the positive cloud feedback in the equilibrium surface energy budget equation, then (10) becomes

$$\Delta\text{LHF} + \gamma\Delta T \approx 0. \tag{12}$$

Hence, though the Andes drives the subsidence that dries and cools the ocean surface through evaporation, (12) predicts that the net effect is a decrease in the evaporation rate ($\Delta\text{LHF} > 0$), consistent with what we see in Table 1.

The diagnostic relation (11) does not provide information on the importance of the low-cloud feedback, since both Δq and ΔT are affected by it. An approximate estimate of the magnitude of this feedback can be made from the regression coefficients in Figs. 3 and 13 in KH93 by assuming that low-troposphere stability is controlled by SST alone and the cloud radiative forcing is approximately the same at the surface as at the top of the atmosphere. This yields the estimate $\gamma \approx 6.6$ W m^{-2} K^{-1}, which—for typical values of the other negative feedbacks in (9)—would double α_r (e.g., Takahashi 2006). Thus, this feedback can lead to twice the magnitudes of both Δq and ΔT. The importance of low-cloud feedback is also highlighted in the experiment reported in section 3a, in which the feedback is removed.

Assuming (10) to be true, we can make an estimate of the cooling (ΔT) we would expect from the changes in surface latent heat fluxes that resulted from the uncoupled (ANDES_FIXED) run (Fig. 6, right). This cooling would correspond to the case in which nothing but T is allowed to change (i.e., no reorganization of the atmospheric flow). Since by construction T does not change in the uncoupled run, using (4) we can write

$$\Delta\text{LHF} = -L_v C_e \rho U \Delta q, \tag{13}$$

because changes in U are of secondary importance. Placing (13) into (11), we obtain

$$\Delta T = \left(L_v C_e \rho U \frac{\partial q_s}{\partial T}\right)^{-1} \Delta\text{LHF}. \tag{14}$$

From Fig. 6 (right), we can estimate ΔLHF to be ~ -30 W m^{-2}. Using typical values for the other parameters on the rhs of 14, we obtain $\Delta\text{T} \approx -1$ K. This value is a third of what the coupled run (ANDES) produces, which again points to the importance of ocean–atmosphere feedbacks for amplifying the response.

4. Northern Hemisphere forcing

a. Rockies and Himalaya

Although the influence of the Rocky and Himalaya mountain ranges on upper-tropospheric flow, in particular their role on forcing stationary eddies, has been extensively studied (see Held et al. 2002, for a review), their influence on the near-surface conditions, which control air–sea interactions in the tropical Pacific, is not obvious.

To assess the influence of the presence of the Rocky and Himalaya mountain ranges on the asymmetry in the tropical Pacific, an experiment [Andes–Rockies–Himalayas (ARH)] was carried out in which these ranges were included in addition to the Andes, as described in section 2a (see Fig. 2).

Adding the Rockies and Himalaya results in the intensification of the North Pacific subtropical anticyclone. This simulation has two anticyclonic center results (Fig. 11, bottom), whereas observations indicate a single, weaker, anticyclonic center on the eastern side of the basin (Fig. 1, bottom).

The stronger anticyclonic circulation has a cooling effect on local SST in the northeast Pacific that is similar to that produced by the Andes in the southeast Pacific (ANDES run). However, despite the apparent overestimation of this effect, it is not strong enough to reverse the north–south asymmetry forced by the Andes in the Pacific, and the ITCZ remains predominantly in the NH east of the date line, although it shifts to the SH farther to the west (cf. Figs. 9 and 11).

We propose that the forcing in the NH is ineffective in altering the north–south asymmetry because of the longitudinal offset between the forced surface cooling in both hemispheres. This hypothesis will be elaborated on and tested in the following section.

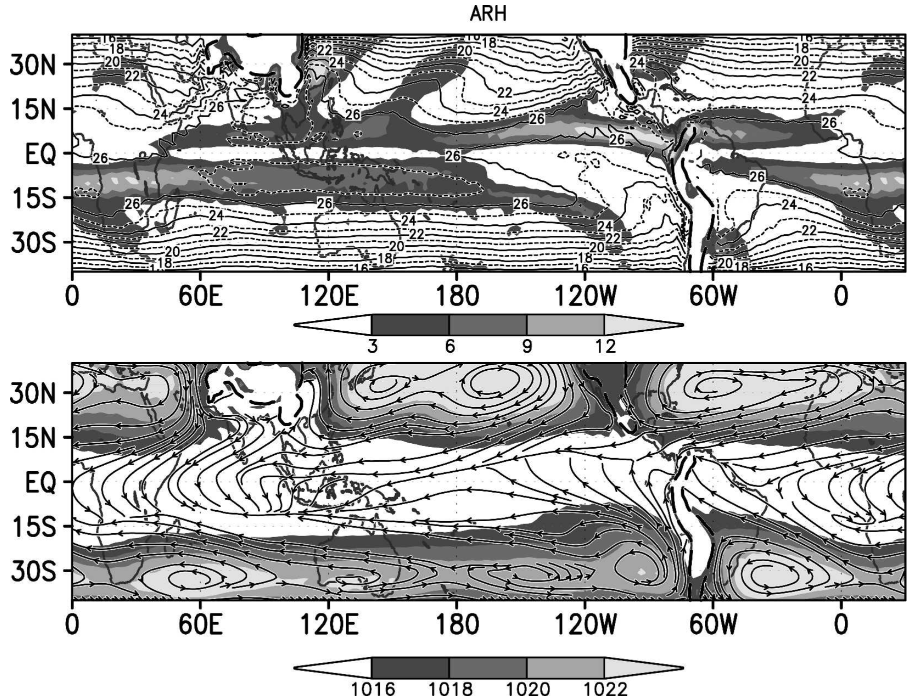

FIG. 11. Same as in Fig. 9, but for the ARH run.

b. Longitudinal offset

The spatial distribution of orography around the Pacific is such that, east of 120°W, the anticyclonic circulation in the North Pacific does not directly affect the near-equatorial Pacific, so the asymmetry in this region is set only by the Andes, whereas, farther to the west, as the north–south asymmetry propagates westward (Xie 1996), the orography in both hemispheres has a direct influence on the asymmetry. We argue that, assuming the forcings in both hemispheres have the same magnitude, the asymmetry will be dominated by the forcing farthest to the east ("upstream").

To test this hypothesis, an experiment was carried out (2ANDES) in which the Andes (as represented in the ANDES experiment but cropped at 5°S) were mirrored about the equator into the NH, to produce equatorially symmetric topography with Andes in both hemispheres, and then the NH Andes were longitudinally shifted by approximately 40° to the west, roughly to the longitude of the Rockies. This experiment was designed to produce a forcing in the NH, a proxy for the Rockies and Himalayas, but eliminating the interhemispheric differences in the shapes of the mountains (i.e., the relative "strengths" of the forcings).

The results show that the NH Andes have a similar local effect over the ocean to the west as their SH counterpart, enhancing the equatorward flow and lowering the underlying SST by approximately the same amounts near 20° latitude (Fig. 12, top and bottom). However, in the Pacific the ITCZ remains north of the equator and the near-equatorial (within 20° latitude) SST remains lower, south of the equator (Fig. 12, top), in support of our hypothesis. Therefore, the fact that the Andes are situated to the east of the Rockies probably plays an important role in the maintenance of the ITCZ north of the equator west of 120°W.

c. Ocean heat transport

A detailed inspection of the observed zonally integrated convergence of the meridional ocean heat transport depicted in Fig. 3 shows some asymmetry with respect to the equator. Between 15° and 45° latitude, there is an average of 16 W m^{-2} less energy going into the ocean in the NH than in the SH, which is a consequence of evaporative and sensible heat fluxes due to airflow over the Kuroshio off the east coast of Asia. This asymmetry can be considered a result of continental geometry.

To assess whether the heat transport asymmetry associated with the Kuroshio can force a north–south asymmetry comparably to the Andes, an experiment was carried out in which the asymmetry in the observed oceanic meridional heat transport convergence (Fig. 3) was added to the Q-fluxes between 15° and 45° latitude in both hemispheres (warming in NH, cooling in SH) at all longitudes. The orographic setup was similar to that

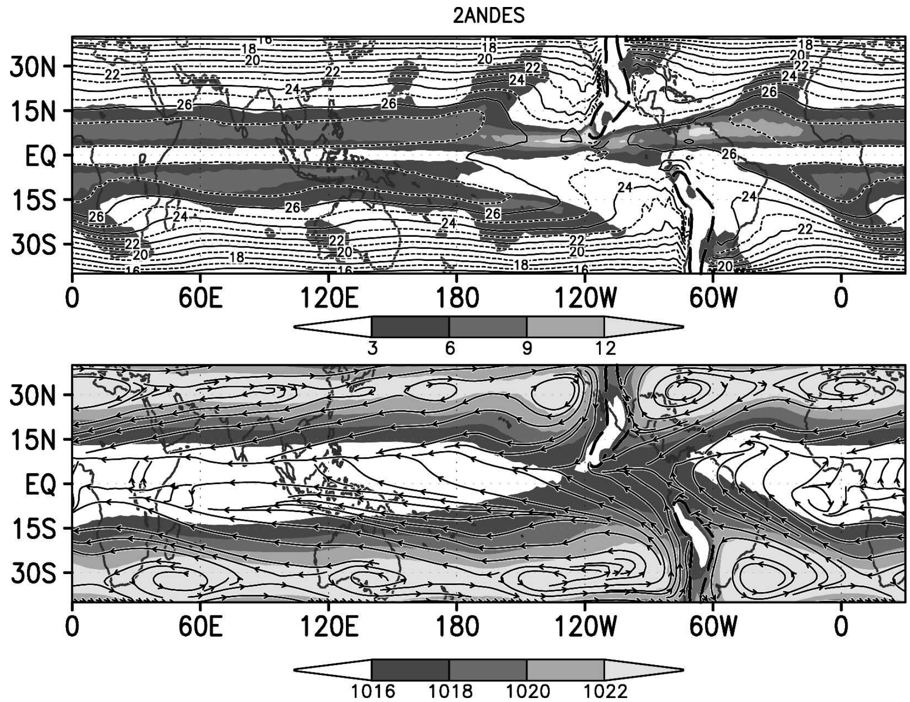

FIG. 12. Same as in Fig. 9, but for the 2ANDES run.

of the ARH experiment, but the Andes were removed. In this way, we can test whether the Kuroshio forcing is comparable to that due to the Andes.

The results (not shown) indicate that the ocean forcing can significantly reduce the strength of the forcing due to the Rockies and the Himalaya, although it is not enough to prevent the ITCZ from remaining in the SH. Therefore, this asymmetry in ocean heat transport appears to be a contributing factor to the tropical north–south asymmetry in the tropical Pacific, but of secondary importance relative to the Andes.

5. Other experiments

a. *Importance of low-cloud feedback*

To assess the importance of the low-cloud feedback in the north–south asymmetry driven by the ANDES, we performed an experiment (ARH+NOSTRATUS) with the same setup as ARH but without the low-cloud parameterization (i.e., with the original cloud scheme of SPEEDY only). The Q-fluxes were recalculated, as in section 2b, from an aquaplanet run similar to AQUA but without the low-cloud parameterization scheme.

The results are quite different. The forcing by the Andes is not able to drive the asymmetry in the east Pacific. In fact, the forcing from the NH orography, particularly the Rockies, creates NH subtropical highs and northeasterly trades that are even stronger than in the ARH experiment. As a result, the ITCZ in the central Pacific is now in the SH (Fig. 13). Yet, the forcing by the Andes is able to maintain a double ITCZ structure in the east Pacific (out to 120°W), whereas a single ITCZ is found south of the equator elsewhere (Fig. 13). Although, admittedly, the NH forcing is unrealistically strong in this model, this result highlights the need to adequately depict the low-cloud feedback, in agreement with current views on the subject (e.g., Mechoso et al. 1995).

b. *Equatorial cold tongue and the east–west asymmetry*

The experiments with realistic mountain forcings feature a strong north–south asymmetry and an east–west contrast, albeit with a zonal SST gradient that is too weak in the equatorial Pacific (~2 K) compared to observations (~5 K). This is most likely the result of the absence of equatorial ocean dynamics in our model, which is essential for coupled ocean–atmosphere processes that strongly contribute to the observed zonal asymmetry (Dijkstra and Neelin 1995).

The presence of a dynamically induced equatorial cold tongue over the eastern Pacific would presumably favor the occurrence of deep atmospheric convection in the equatorial west Pacific, which is something the

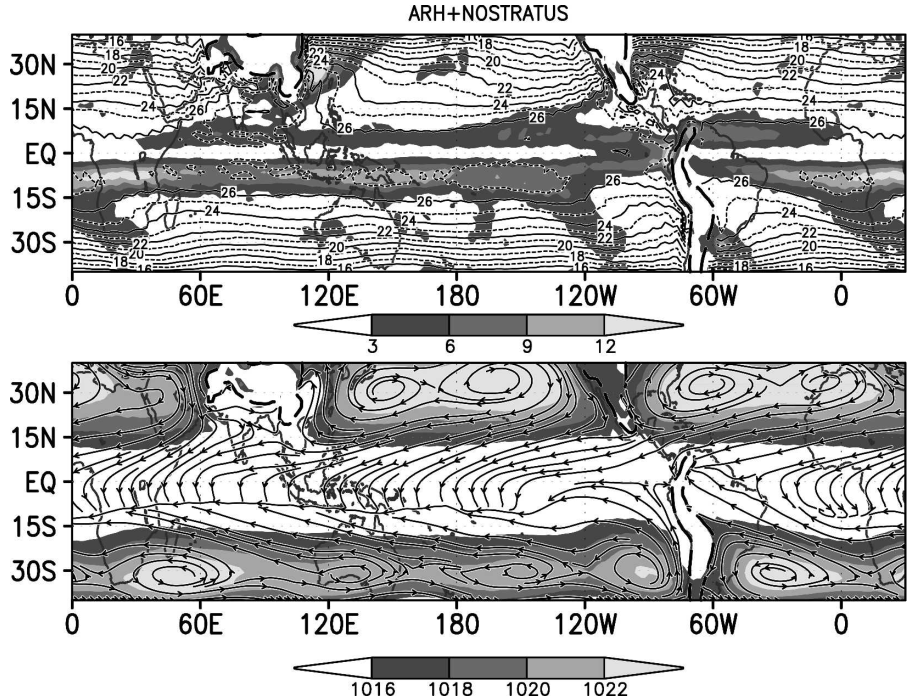

FIG. 13. Same as in Fig. 9, but for the ARH+NOSTRATUS run.

aforementioned experiments lacked. On the other hand, the presence of a stronger cold tongue can have a symmetrizing effect in the eastern Pacific by driving low-level convergence south of the equator (Lietke et al. 2001; Gu et al. 2005).

To test the effect of a more realistic east–west asymmetry with a stronger equatorial cold tongue, a run (ARH + CT) was carried out with the same configuration as the ARH run, but with a perturbation added to the Q-fluxes as a proxy for the effect of the thermocline tilt on equatorial upwelling. This perturbation was calculated by fitting a sine function in longitude between 120°E and 80°W to the annual mean surface net heat fluxes from the Southampton Oceanography Centre (SOC) dataset (Josey et al. 1999) within 10° of the equator, and then symmetrizing the result with respect to the equator. The resulting perturbation has a peak-to-peak amplitude of 64 W m^{-2} at the equator (Fig. 14).

The results feature a well-defined east Pacific cold tongue (Fig. 15), although considerably farther to the west than observed (cf. Fig. 1). The total east–west difference in SST is around 4 K, which is closer than in the ARH run to the observed. Furthermore, the results feature deep convection on the equator between 120° and 160°E, which was absent in the ARH run, although the western Pacific warm pool is smaller than observed.

The modeled equatorial cold tongue is strong enough

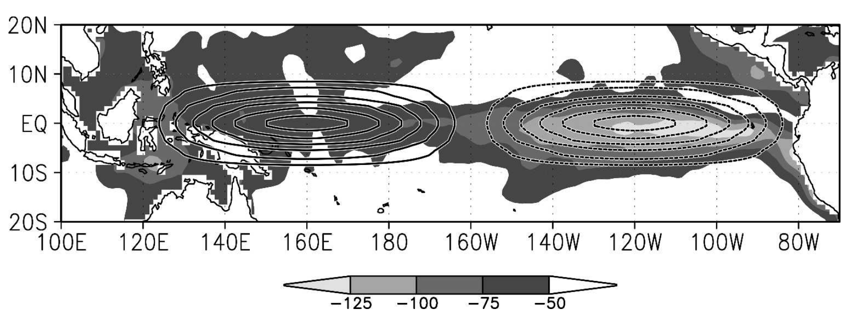

FIG. 14. Observed annual mean Q-flux (−1 × SOC net surface heat flux; W m^{-2}; shaded) and the Q-flux perturbation used in the ARH+CT run (contours; interval 5 W m^{-2}; zero omitted, negative dashed).

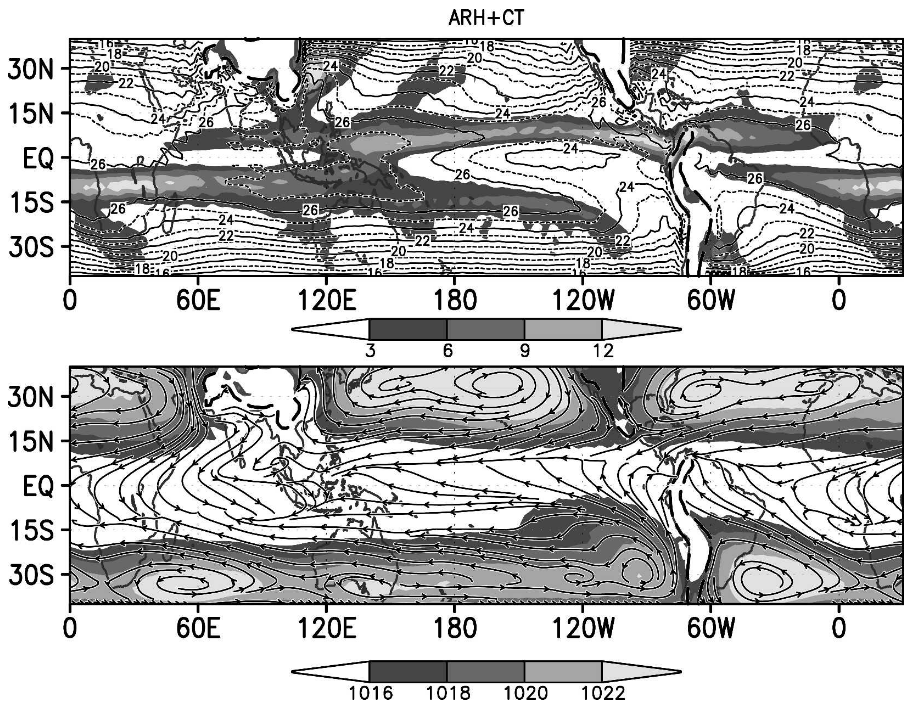

FIG. 15. Same as in Fig. 9, but for the ARH+CT run.

to produce southward SST gradients between the equator and 5°S east of 120°W (Fig. 15). Such gradients cause low-level convergence south of the equator through thermally induced pressure gradients (Lindzen and Nigam 1987), which could lead to an ITCZ in the SH, as mentioned previously. Indeed, the 925-mb divergence is reduced by around 5×10^{-7} s^{-1} (20%) near 5°S between 130° and 90°W, but not enough to promote deep convection. However, it is possible that a stronger cold tongue or a convective parameterization scheme that is more sensitive to low-level moisture convergence could lead to a double ITCZ configuration.

c. *Seasonal cycle*

Giese and Carton (1994) showed that the seasonal cycle of insolation could have a profound effect on the mean state if the seasonality in SST in the SH were strong enough to reverse the north–south asymmetry during the warm season, which would lead to an annual mean state featuring a double ITCZ.

To test the robustness to seasonality of the north–south asymmetry forced by the Andes, a run (ARH + CT + SEAS) was performed with the same configuration as the ARH + CT experiment, except that the insolation was allowed to vary seasonally, with zero orbital eccentricity. By construction, the annual mean incident insolation at the top of the atmosphere was the same as in the previous experiments.

The resulting mean state from this run (not shown) is similar to the one from the ARH + CT run. The modeled seasonal cycle was similar to the observed, albeit weaker (not shown). In the southeast Pacific, this weakness might be due to an underestimation of the low-cloud/SST feedback in the model (Takahashi 2005).

The north–south asymmetry is essentially unaffected by the introduction of the seasonal cycle. Both the mean ITCZ and SPCZ are displaced slightly toward the poles, and the eastern Pacific is cooler (by around 1 K). The rainfall rate in the ITCZ is less than in the ARH + CT run, due to seasonal meridional displacements of the eastern Pacific ITCZ of around 5° latitude, and a weakening during March and April, when it is closest to the equator. Some rainfall does occur south of the equator (around 4°S) between March and May, but it is smaller than that in the NH at that time and the annual mean rainfall distribution does not feature a double ITCZ.

d. *Equatorial ITCZ*

The establishment of the north–south asymmetry in our experiments can be described as the eradication, in the eastern Pacific, of the southern branch of the double ITCZ found in the reference state. To test whether our results depend on having this double ITCZ configuration in the reference state, we performed two experiments. The first experiment (AQUA_EQ) is a prescribed SST aquaplanet run with the same setting as the AQUA run, except that a perturbation was added to the reference SST to remove the equatorial minimum (i.e., the cold tongue) and make it a maximum. This resulted in a zonal mean climate with a strong single ITCZ located on the equator (not shown). The results from the AQUA_EQ run were then used to determine the Q-fluxes for a coupled experiment (ARH_EQ), which is otherwise the same as the ARH run (i.e., includes the Andes, the Rockies, and the Himalayas). The results feature a significant asymmetry in the eastern Pacific out to 160°W (not shown), albeit unsurprisingly weaker than in the ARH run. In particular, the eastern Pacific ITCZ is located around 3°N, while the southeastern Pacific is cooled by around 2°C (the respective numbers for the ARH run were about 6°N and 3.5°C). This experiment shows that the Andes are sufficient to establish the north–south asymmetry in the eastern Pacific from a reference state without an equatorial cold tongue and with a single equatorial ITCZ, even in the presence of the Rockies and Himalayas.

6. Discussion

The evaporative cooling associated with large-scale subsidence appears to play a major role in producing the relatively low temperatures seen off the western coast of South America, causing the ITCZ to reside in the NH. In the tropical Atlantic and Indian Oceans, mountain forcing is probably secondary in importance to land–sea thermal contrasts in determining the north–south asymmetries. However, the ocean cooling by the dry subsidence associated with subtropical anticyclones is likely to be at work.

Given that our model has a crude representation of boundary layer processes, one might question whether the drying mechanism, which depends on the entrainment of subsiding air into the boundary layer, can efficiently occur in nature. The observationally based estimates of entrainment rates at the boundary layer top in the stratus region in the southeast Pacific are around 3–4 mm s^{-1}, or about 0.04 Pa s^{-1} (Wood and Bretherton 2004; Caldwell et al. 2005); in equilibrium, the entrainment rate must be balanced by the subsidence rate, which in our model is $\sim$0.05 Pa s^{-1}. Hence, we believe that our model is adequately representing the importance of this process.

The WES mechanism proposed by Xie and Philander (1994), by which air–sea interactions reinforce an asymmetric state with the ITCZ in one hemisphere, is a useful concept for explaining our results. However, additional aquaplanet experiments indicate that the asymmetric (symmetric) state in our model is not as stable (unstable) as in theirs. This is partly the consequence of cloud radiative effects, namely shortwave shading by convective clouds, which in our model (and presumably in nature) vary in opposition to changes in evaporative cooling. Thus, our results suggest that the WES mechanism (Xie and Philander 1994) might be more fruitfully considered as a feedback that enhances the response to asymmetric forcing, such as that by the Andes, and not as a strong symmetry-breaking mechanism in its own right.

Our results are not inconsistent with other recent studies dealing with the effect of orography, particularly the Andes, on the eastern Pacific climate. Kitoh (2002) examined the contributions of the (global) orography to the climate simulated using the MRI flux-corrected coupled ocean–atmosphere GCM, and his results show a response in the tropical Pacific to the presence of mountains that is consistent with ours, although the flux correction precluded the appreciation of the full impact of the removal of the Andes in their experiment. A similar issue arises with the study by Xu et al. (2004), who removed the Andes in an experiment with a regional atmospheric model with prescribed SST and argued that the presence of the Andes favored low-level clouds in the southeast Pacific by blocking warm advection from the east. Although their results are consistent with our interpretation, their experimental design (fixed SST that already included the subsidence-induced cooling) did not enable them to identify the most important effect of the Andes.

It is interesting to note that the presence of the South American landmass, even in the absence of the Andes, can lead to a north–south asymmetry, albeit much weaker than that produced by the Andes, due to the dryness of the easterly flow entering the southeast Pacific. This was observed in an experiment at T30 resolution with idealized landmasses and the interactive ocean mixed layer. We believe that this process, rather than coastal upwelling, could have been responsible for the (weak) asymmetry found by Philander et al. (1996) in their experiments.

The annual cycle in upper-ocean heat content in the southeast tropical Pacific, which is closely related to SST (Takahashi 2005), is dominated by the seasonality of insolation, which is strongly enhanced by a feedback involving low-level clouds (Mitchell and Wallace 1992; Takahashi 2005). The similarity between the spatial pattern of the annual mean reduction of SST due to the Andes (Fig. 10) and the pattern of the climatological May to August transition in SST (Fig. 7 in Mitchell and Wallace 1992) is probably not a coincidence, as the low-cloud feedback that enhances the annual cycle of SST will be more effective where the annual mean SST is low because of the Andes. This is because low SST implies high low-level stability, which favors the presence of the low-level clouds (KH93).

7. Summary and conclusions

The hypothesis that the distribution of orography determines the north–south asymmetry in the tropical Pacific through atmosphere-only processes was tested by performing experiments with an atmospheric general circulation model coupled to an idealized model of the ocean with no built-in asymmetries, either in the east–west or the north–south directions.

We showed that subsidence of low specific humidity air to the west of the Andes exerts a strong local control on SST through evaporation. The presence of the Andes is found to be sufficient for generating such a circulation, in agreement with Rodwell and Hoskins (2001), and the associated surface cooling is sufficient to create a north–south asymmetry, with the ITCZ in the Northern Hemisphere in the east Pacific, through feedbacks involving air–sea interactions (WES feedback; Xie and Philander 1994).

Furthermore, we showed that despite the existence of similar processes in the North Pacific due to anticyclonic flow forced by the Himalayas and Rockies, the fact that the Andes are located farther to the east than any of these ranges allows the Andes to set the north–south asymmetry, which then propagates westward into the Pacific (Xie 1996).

The north–south asymmetry forced by the Andes appears to be robust to the presence of an equatorial cold tongue and to the seasonality in insolation. It was also found that north–south asymmetries in ocean heat transport (associated with the Kuroshio) are of secondary importance, but that can contribute to reinforcing the asymmetry.

Some simple calculations and a numerical experiment indicate that the feedback involving low-cloud cover and SST (Mitchell and Wallace 1992; Philander et al. 1996) plays a significant role in enhancing the cooling off South America driven by the Andes and allowing the associated north–south asymmetry to dominate in the Pacific. It should be noted that processes other than those addressed in this paper, such as upwelling along the coast of South America, feedbacks between low-level clouds and meridional winds (Nigam 1997; Wang et al. 2005), and summertime convection in the Amazon (Rodwell and Hoskins 2001), may play a secondary role in reinforcing the asymmetry.

Current state-of-the-art coupled ocean–atmosphere general circulation models still have problems representing the observed north–south asymmetry (e.g., Mechoso et al. 1995). Despite different physical parameterization schemes (e.g., convective and boundary layer) and different representations of the ocean processes, the physical processes by which the presence of the Andes cools the southeast tropical Pacific are likely to be robust and reproducible in other models as long as the interaction between the zonal mean flow and the Andes and the humidity of the subsiding air are adequately represented. It should be noted, however, that the preparation of the orography used in this study emphasized the preservation of the height of the Andes to ensure that the nonlinear interaction with the zonal mean flow (Rodwell and Hoskins 2001) was well represented, which is not a common practice in climate modeling. We will pursue collaborations with other modeling groups to assess the reproducibility and robustness of these results.

Acknowledgments. This study is part of the doctoral dissertation of KT. The authors thank C. S. Bretherton, T. P. Mitchell, J. M. Wallace, R. Wood, and three anonymous reviewers for useful comments and suggestions.

APPENDIX

Low-Level Cloud Scheme

Low-level stability is diagnosed similarly to KH93:

$$\Delta\theta = \theta(\sigma = 0.685) - \theta(\text{surface}) + 5\ \text{K},$$

where θ is potential temperature and the addition of 5 K is a correction for the low vertical resolution of the model, while $\sigma = p/p_s$, where p_s is surface pressure, is the vertical coordinate of the model.

Stratiform CC is placed over the ocean where $\Delta\theta >$ 14 K, where there is subsidence at $\sigma = 0.685$, and where the diagnosed stratus cloud cover would be higher than that predicted by the original cloud scheme. In that case, stratus clouds would be placed between $\sigma = 0.77$ and $\sigma = 0.60$, with CC (in %) calculated following the linear relation found by KH93:

$$\text{CC} = 5.7\Delta\theta - 55.73.$$

This diagnosed cloud cover is used only for the shortwave calculations and does not directly affect the moisture distribution.

REFERENCES

Caldwell, P., C. S. Bretherton, and R. Wood, 2005: Mixed-layer budget analysis of the diurnal cycle of entrainment in southeast Pacific stratocumulus. *J. Atmos. Sci.,* **62,** 3775–3791.

Dijkstra, H. A., and J. D. Neelin, 1995: Ocean–atmosphere interaction and the tropical climatology. Part II: Why the Pacific cold tongue is in the east. *J. Climate,* **8,** 1343–1359.

Giese, B. S., and J. A. Carton, 1994: The seasonal cycle in a coupled ocean–atmosphere model. *J. Climate,* **7,** 1208–1217.

Gu, G., R. F. Adler, and A. H. Sobel, 2005: The eastern Pacific ITCZ during the boreal spring. *J. Atmos. Sci.,* **62,** 1157–1174.

Hartmann, D. L., and M. L. Michelsen, 1993: Large-scale effects on the regulation of tropical sea surface temperature. *J. Climate,* **6,** 2049–2062.

Held, I. M., and P. J. Phillips, 1993: Sensitivity of the eddy momentum flux to meridional resolution in atmospheric GCMs. *J. Climate,* **6,** 499–507.

——, M. Ting, and H. Wang, 2002: Northern winter stationary waves: Theory and modeling. *J. Climate,* **15,** 2125–2144.

Huffman, G. J., and Coauthors, 1997: The Global Precipitation Climatology Project (GPCP) combined precipitation dataset. *Bull. Amer. Meteor. Soc.,* **78,** 5–20.

Kalnay, E., and Coauthors, 1996: The NCEP/NCAR 40-Year Reanalysis Project. *Bull. Amer. Meteor. Soc.,* **77,** 437–471.

Kistler, R., and Coauthors, 2001: The NCEP–NCAR 50-Year Reanalysis: Monthly means CD-ROM and documentation. *Bull. Amer. Meteor. Soc.,* **82,** 247–267.

Kitoh, A., 2002: Effects of large-scale mountains on surface climate—A coupled ocean-atmosphere general circulation model study. *J. Meteor. Soc. Japan,* **80,** 1165–1181.

Klein, S. A., and D. L. Hartmann, 1993: The seasonal cycle of low stratiform clouds. *J. Climate,* **6,** 1587–1606.

Josey, S. A., E. C. Kent, and P. K. Taylor, 1999: *The Southampton Oceanography Centre* (*SOC*) *Ocean–Atmosphere Heat, Momentum and Freshwater Flux Atlas.* Southampton Oceanography Centre, Southampton, United Kingdom, 30 pp. plus figures.

Lietzke, C. E., C. Deser, and T. H. Vonder Haar, 2001: Evolutionary structure of the eastern Pacific double ITCZ based on satellite moisture profile retrievals. *J. Climate,* **14,** 743–751.

Lindzen, R. S., and S. Nigam, 1987: On the role of sea surface temperature gradients in forcing low-level winds and convergence in the tropics. *J. Atmos. Sci.,* **44,** 2418–2436.

Mechoso, C. R., and Coauthors, 1995: The seasonal cycle over the tropical Pacific in coupled ocean–atmosphere general circulation models. *Mon. Wea. Rev.,* **123,** 2825–2838.

Mitchell, T. P., and J. M. Wallace, 1992: The annual cycle in equatorial convection and sea surface temperature. *J. Climate,* **5,** 1140–1156.

Molteni, F., 2003: Atmospheric simulations using a GCM with simplified physical parameterizations. I: Model climatology and variability in multi-decadal experiments. *Climate Dyn.,* **20,** 175–191.

Nigam, S., 1997: The annual warm to cold phase transition in the eastern equatorial Pacific: Diagnosis of the role of stratus cloud-top cooling. *J. Climate,* **10,** 2447–2467.

Philander, S. G. H., D. Gu, D. Halpern, G. Lambert, N.-C. Lau, T. Li, and R. C. Pacanowski, 1996: Why the ITCZ is mostly north of the equator. *J. Climate,* **9,** 2958–2972.

Reynolds, R. W., N. A. Rayner, T. M. Smith, D. C. Stokes, and W. Wang, 2002: An improved in situ and satellite SST analysis for climate. *J. Climate,* **15,** 1609–1625.

Riehl, H., 1979: *Climate and Weather in the Tropics.* Academic Press, 611 pp.

Rodwell, M. J., and B. J. Hoskins, 2001: Subtropical anticyclones and summer monsoons. *J. Climate,* **14,** 3192–3211.

Takahashi, K., 2005: The annual cycle in the Peru Current region. *J. Climate,* **18,** 4937–4954.

——, 2006: Processes controlling the tropical Pacific mean precipitation pattern. Ph.D. dissertation, University of Washington, 135 pp.

——, and D. S. Battisti, 2007: Processes controlling the mean tropical Pacific precipitation pattern. Part II: The SPCZ and the Southeast Pacific Dry Zone. *J. Climate,* in press.

Trenberth, K. E., and J. M. Caron, 2001: Estimates of meridional atmosphere and ocean heat transports. *J. Climate,* **14,** 3433–3443.

Wang, B., and Y. Wang, 1999: Dynamics of the ITCZ–equatorial cold tongue complex and causes of the climate asymmetry. *J. Climate,* **12,** 1830–1847.

Wang, Y., S.-P. Xie, B. Wang, and H. Xu, 2005: Large-scale atmospheric forcing by southeast Pacific boundary layer clouds: A regional model study. *J. Climate,* **18,** 934–951.

Wood, R., and C. S. Bretherton, 2004: Boundary layer depth, entrainment and decoupling in the cloud-capped subtropical and tropical marine boundary layer. *J. Climate,* **17,** 3576–3588.

Xie, S.-P., 1996: Westward propagation of latitudinal asymmetry in a coupled ocean–atmosphere model. *J. Atmos. Sci.,* **53,** 3236–3250.

——, and S. G. H. Philander, 1994: A coupled ocean-atmosphere model of relevance to the ITCZ in the eastern Pacific. *Tellus,* **46A,** 340–350.

——, and K. Saito, 2001: Formation and variability of a northerly ITCZ in a hybrid coupled AGCM: Continental forcing and oceanic–atmospheric feedback. *J. Climate,* **14,** 1262–1276.

Xu, H., Y. Wang, and S.-P. Xie, 2004: Effect of the Andes on eastern Pacific climate: A regional atmospheric model study. *J. Climate,* **17,** 589–602.